On the decomposition of foliar hyperspectral signatures for the high-fidelity discrimination and monitoring of crops

Gladimir V. G. Baranoski[a], Spencer Van Leeuwen[a] and Tenn F. Chen[a],

[a]Natural Phenomena Simulation Group, School of Computer Science, University of Waterloo, 200 University Avenue West, Waterloo, Canada

ABSTRACT

Hyperspectral technologies are being increasingly employed in precision agriculture. By separating the surface and subsurface components of foliar hyperspectral signatures using polarization optics, it is possible to enhance the remote discrimination of different plant species and optimize the assessment of different factors associated with the crops' health status such as chlorophyll levels and water content. These initiatives, in turn, can lead to higher crop yield and lower environmental impact through a more effective use of freshwater supplies and fertilizers (reducing the risk of nitrogen leaching). It is important to consider, however, that the main varieties of crops, represented by C_3 (*e.g.*, soy) and C_4 (*e.g.*, maize) plants, have markedly distinct morphological characteristics. Accordingly, the influence of these characteristics on their interactions with impinging light may affect the selection of optimal probe wavelengths for specific applications making use of combined hyperspectral and polarization measurements. In this work, we compare the sensitivity of the surface and subsurface reflectance responses of C_3 and C_4 plants to different spectral and geometrical light incidence conditions. In our comparisons, we also consider intra-species variability with respect to specimen characterization data. This investigation is supported by measured biophysical data and predictive light transport simulations. The results of our comparisons indicate that the surface and subsurface reflectance responses of C_3 and C_4 plants depict well-defined patterns of sensitivity to varying illumination conditions. We believe that these patterns should be considered in the design of new high-fidelity crop discrimination and monitoring procedures.

Keywords: foliar optical properties, surface reflectance, subsurface reflectance, polarization, simulation.

1. INTRODUCTION

Plants are considered primary remote sensing targets due to their importance to sustain human and animal life. Not surprisingly, there has been a vast body of work devoted to the acquisition and analysis of plants' spectral data as well as to the modeling of their interactions with light at different scales, from individual leaves and canopies to entire landscapes covered by vegetation[1]. For the success of these applications, it is essential that stress factors, such as water and nutrient losses, can be effectively detected and timely addressed. These factors can result in changes in how plants absorb, transmit and reflect light. Accordingly, the spectral signatures of their leaves can be used as physiological-status indicators and assist in the mitigation of the adverse effects triggered by the stress factors. These connections provide the basis for the increasing use of hyperspectral technology in the remote sensing of crops[2–4].

Stress factors affecting the physiological status of plants tend to have a dominant impact on the subsurface (diffuse) component of their reflectance since the surface (specular) component represents light that does not penetrate their foliar tissues. Using hyperspectral devices combined with polarization optics, one can perform examinations of changes in foliar subsurface reflectance[5,6], which, in turn, can potentially lead to more precise stress assessments. However, it is important to consider that the main varieties of cultivated plants belonging to the C_3 and C_4 groups have distinct morphological characteristics that can affect their hyperspectral responses[7].

In this paper, we investigate the sensitivity of C_3 and C_4 plants' total reflectance (including surface and subsurface components) and subsurface reflectance to different illumination conditions. More specifically, we consider two species representative of these groups, namely soy (*Soja hispida*) and maize (*Zea mays*, commonly

Further author information: (Send correspondence to Gladimir V. G. Baranoski)
Gladimir V. G. Baranoski: E-mail: gvgbaran@cs.uwaterloo.ca

Multispectral, Hyperspectral, and Ultraspectral Remote Sensing Technology, Techniques and Applications VI, edited by Allen M. Larar, Prakash Chauhan, Makoto Suzuki, Jianyu Wang, Proc. of SPIE Vol. 9880, 98800G
 · doi: 10.1117/12.2223806

known as corn) respectively. While the former is characterized by bifacial leaves, the latter is characterized by unifacial leaves. We note, however, that there are C_3 species characterized by unifacial leaves[8] and C_4 species characterized by bifacial leaves[9]. Our investigation is based on *in silico* experiments in which we simulated light interactions with different leaf specimens representative of these two species. In these experiments, the specific morphological characteristics of soy and maize leaves were taken into account. Comparing the simulation results obtained for these two species, one can observe trends that should be taken into consideration by initiatives aimed at the interpretation of plants' hyperspectral responses. We remark that the higher the reliability of these interpretations, the higher the fidelity of procedures for the discrimination and monitoring of crops using remote sensing technology.

2. MATERIALS AND METHODS

2.1 Simulation Framework Overview

Our *in silico* experiments were performed using predictive hyperspectral models of light interaction with bifacial and unifacial plant leaves, namely ABM-B (algorithmic BDF (bidirectional scattering distribution function) model for bifacial plant leaves) and ABM-U (algorithmic BDF model for unifacial plant leaves) respectively[10,11]. In order to allow the reproduction and extension of our investigation to other experimental conditions, we made these models and the supporting biophysical data (*e.g.*, refractive indices and absorption coefficients) employed in this work accessible through our online system[12,13]. Using this system[14], researchers can configure simulation parameters (*e.g.*, wavelength range and angle of incidence) as well as specimen characterization data (*e.g.*, thickness and pigment contents) through web interfaces (Figures 1 and 2), and run the models. For the characterization of typical exemplars of soy and maize leaves, we used measured data[15] and observations reported in the literature[10,16,17]. In Table 1, we provide a summary of the values assigned to these specimens' biophysical parameters during this investigation. Note that we refer to the soy specimens as S1 and S2, and the maize specimens as M1 and M2.

Parameter	S1	S2	M1	M2
Thickness (cm)	0.01660	0.0106	0.0204	0.0224
Mesophyll percentage (%)	50	50	70	70
Chlorophyll A concentration (g/cm^3)	0.00392	0.00605	0.00290	0.00342
Chlorophyll B concentration (g/cm^3)	0.00117	0.00170	0.00070	0.00120
Carotenoids concentration (g/cm^3)	0.00107	0.00167	0.00066	0.00091
Protein concentration (g/cm^3)	0.11064	0.14752	0.05793	0.06656
Cellulose concentration (g/cm^3)	0.01074	0.07900	0.05775	0.07152
Lignin concentration (g/cm^3)	0.01014	0.01361	0.00661	0.00760
Cuticle undulations aspect ratio	5	5	10	10
Epidermal cell caps aspect ratio	5	5	5	5
Palisade cell caps ratio	1	1	-	-
Spongy cell caps aspect ratio	5	5	5	5

Table 1: Parameters employed in the characterization of the soy (S1 and S2) and maize (M1 and M2) specimens. The thickness values and biochemical data assigned to S1, S2, M1 and M2 correspond to the actual characteristics of the soy and maize specimens used to obtain the LOPEX[15] spectral measurements 219, 225, 141 and 537, respectively.

Within the ABM-B and ABM-U ray-optics formulations, a ray interacting with a given leaf specimen can be associated with any selected wavelength within spectral regions of interest in the visible and near-infrared (NIR) domains. Hence, these models can provide reflectance readings with different spectral resolutions. In terms of illumination and collection geometries, these models can provide bidirectional reflectance and transmittance quantities by recording the direction of the outgoing rays using a virtual gonioreflectometer[18,19]. In addition, one can obtain directional-hemispherical reflectance and transmittance quantities by integrating the outgoing rays with respect to the collection hemisphere using a virtual spectrophotometer[19,20]. The modeled curves depicted in this work correspond to directional-hemispherical reflectances obtained from the leaves' adaxial surfaces. In their computation, we considered a spectral resolution of $5nm$ and employed 10^6 sample rays per wavelength.

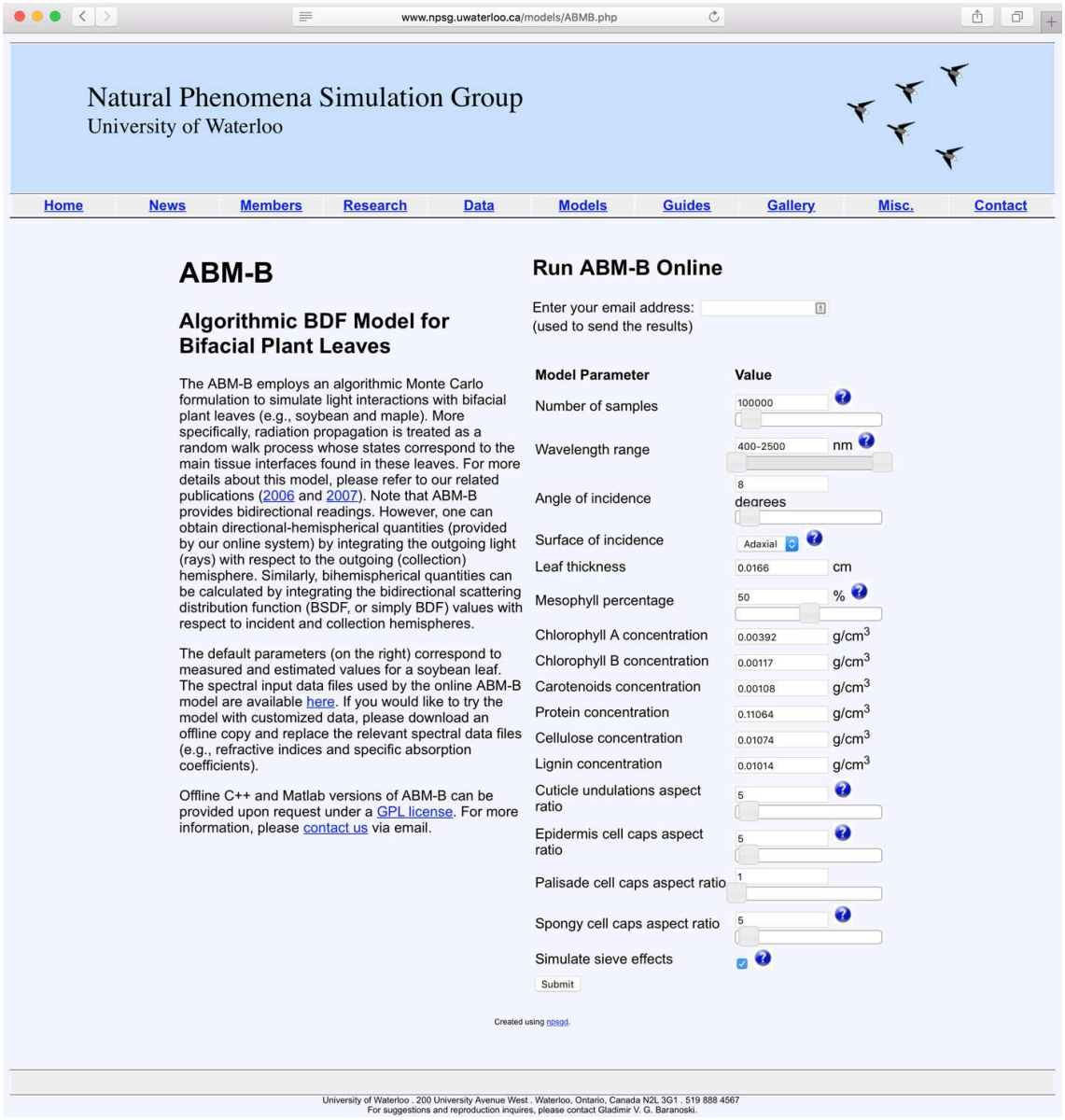

Figure 1: The web interface for the ABM-B model[12] available through the Natural Phenomena Simulation Group Distributed (NPSGD) system[14]. Through this interface, researchers can configure biophysical parameters and execute light transport simulations involving plants characterized by bifacial leaves.

2.2 Sensitivity Analysis

In our experiments, distinct illuminations conditions were simulated by varying the wavelength of the impinging light and the angle of incidence, which is denoted by θ and specified with respect to the specimen's normal. In order to compare the total reflectance and subsurface reflectance of the selected specimens under these conditions, we performed a parameter differential sensitivity analysis[21,22], also known as direct sensitivity analysis method. It consists in the computation of a sensitivity index for a specific parameter. This index, which was introduced by Hoffman and Gardner[23] to account for uncertainties in environmental assessment models, provides the ratio of the change in output to the change in the selected parameter while all other parameters remain fixed. A sensitivity index of 1.0 indicates complete sensitivity (or maximum impact), while a sensitivity index less than 0.01 indicates that the output is insensitive to changes in the parameter[23]. Accordingly, we computed the mean

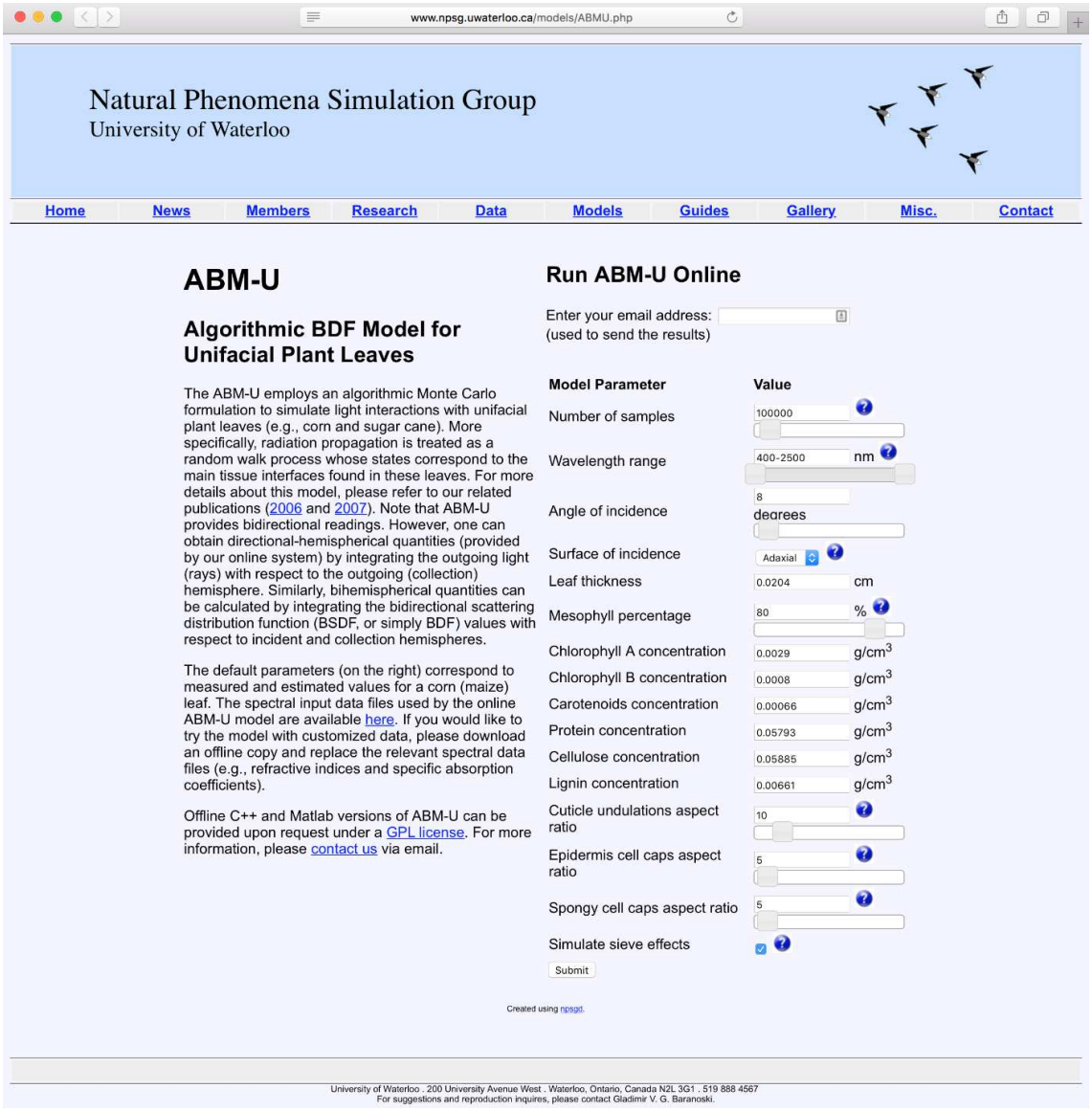

Figure 2: The web interface for the ABM-U model[13] available through the Natural Phenomena Simulation Group Distributed (NPSGD) system[14]. Through this interface, researchers can configure biophysical parameters and execute light transport simulations involving plants characterized by unifacial leaves.

sensitivity index (MSI) for the spectral regions of interest, namely visible (400-700nm), NIR-A (700-1300nm) and NIR-B (1300-2500nm), in order to assess the mean ratio of change in reflectance to the change in the angle of incidence. This index is expressed as:

$$MSI = \frac{1}{N}\sum_{i=1}^{N}\frac{|\rho_0(\lambda_i) - \rho_\theta(\lambda_i)|}{\max\{\rho_0(\lambda_i), \rho_\theta(\lambda_i)\}}, \tag{1}$$

where ρ_0 corresponds to a baseline reflectance curve computed considering $\theta = 0°$, ρ_θ represents a reflectance curve computed considering a specific value assigned to θ, and N is the total number of wavelengths sampled with a $5nm$ resolution within a selected spectral region.

3. RESULTS AND DISCUSSION

The results of our experiments for the soy and maize specimens are presented in Figures 3 and 4 respectively. As expected, as we increase the angle of incidence from 0° to 60°, the total reflectance increases for both groups of specimens due to the stronger contribution of the surface component. Within this angular range, it can also be observed that the variations on subsurface reflectance were substantially less pronounced than the corresponding variations in total reflectance.

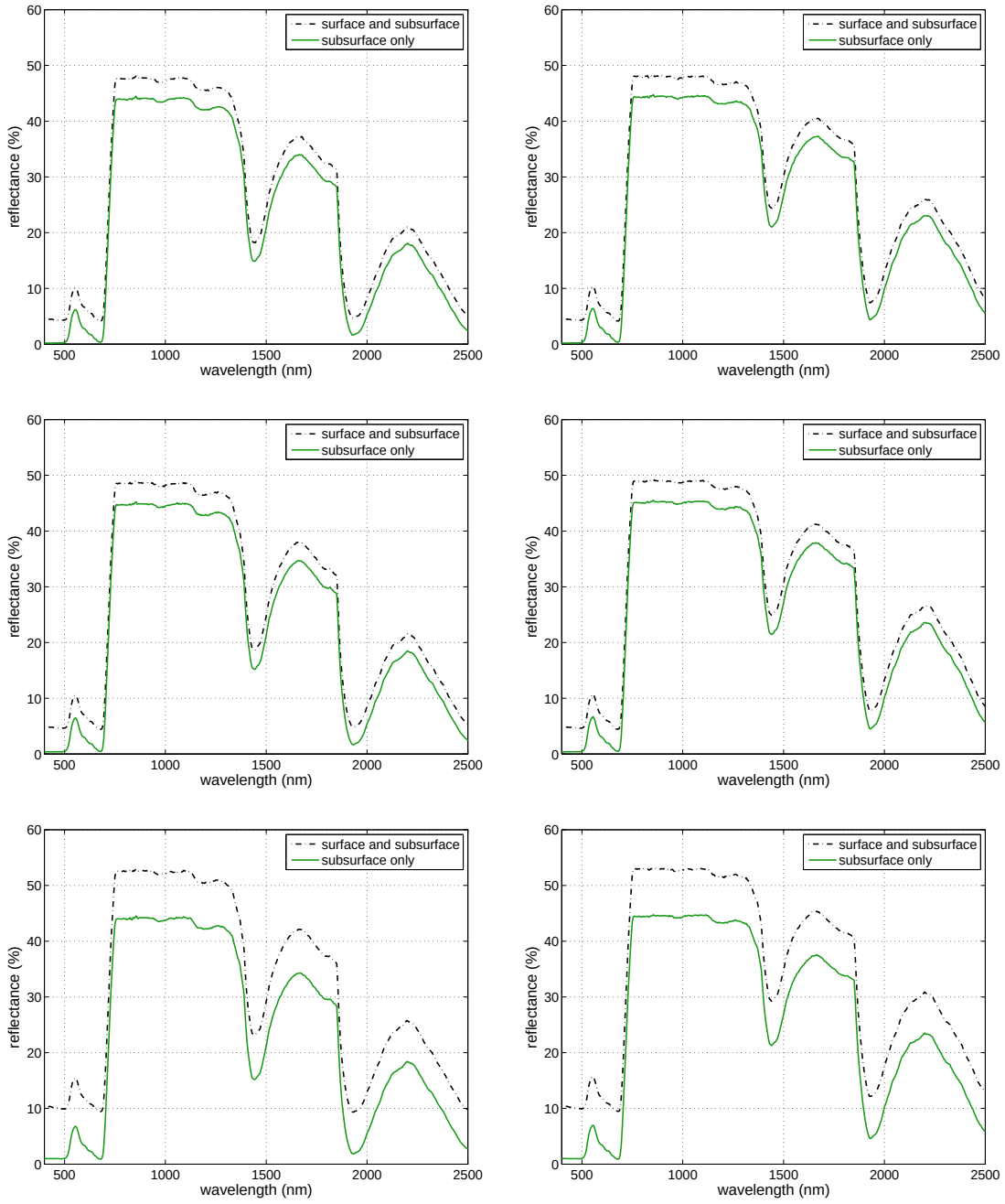

Figure 3: Total reflectance (surface and subsurface components) and subsurface reflectance curves computed for the soy specimens S1 (left) and S2 (right) considering three angles of incidence: 0° (top row), 30° (middle row) and 60° (bottom row). The curves were obtained using the ABM-B model[12] and the data provided in Table 1.

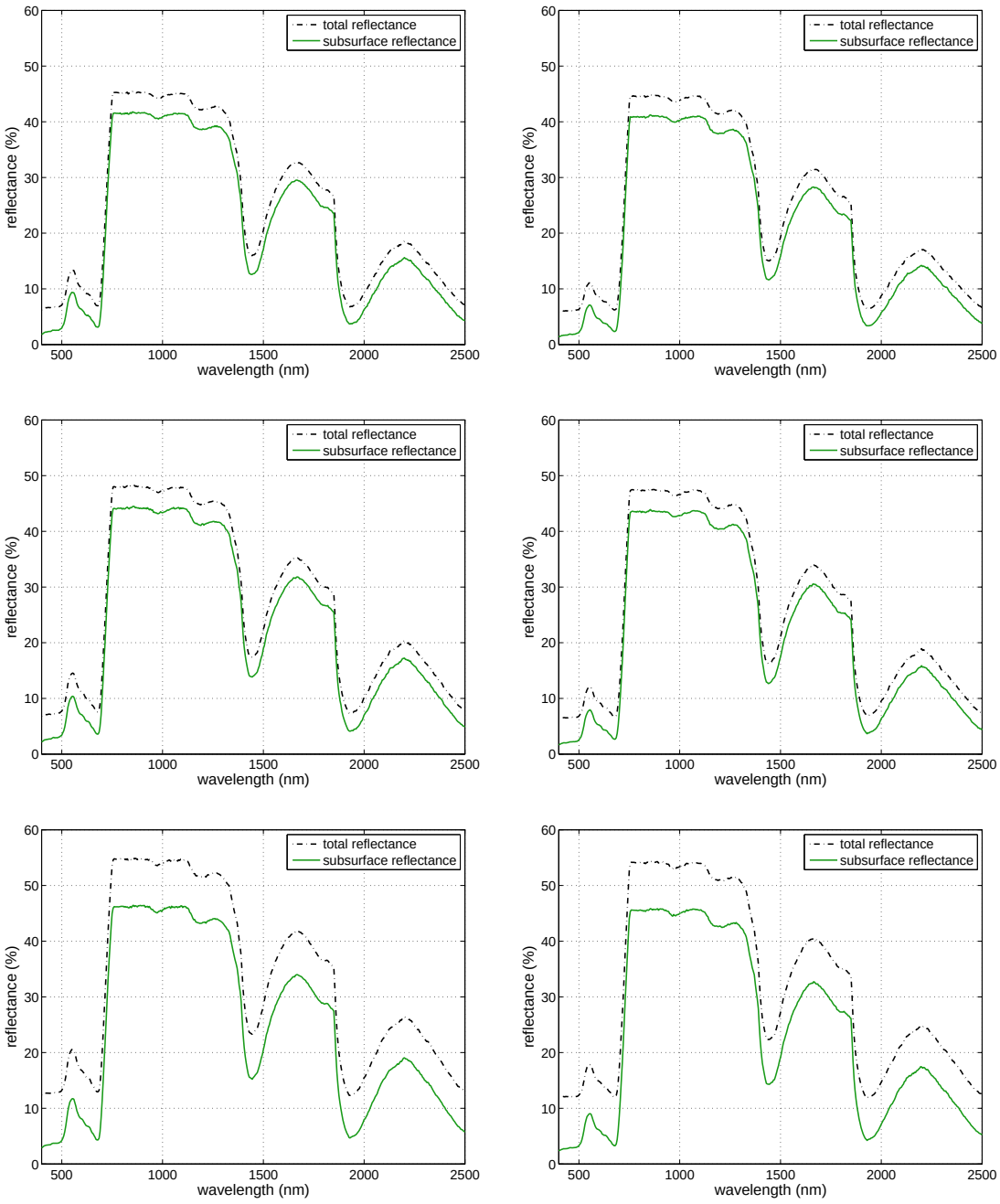

Figure 4: Total reflectance (surface and subsurface components) and subsurface reflectance curves computed for the maize specimens M1 (left) and M2 (right) considering three angles of incidence: 0° (top row), 30° (middle row) and 60° (bottom row). The curves were obtained using the ABM-U model[13] and the data provided in Table 1.

These aspects seem to indicate that the total reflectance and the subsurface reflectance of the bifacial C_3 and unifacial C_4 specimens are characterized by the same behaviour with respect to their dependence on the angle of incidence. However, a closer examination of their behaviours across the visible, NIR-A and NIR-B spectral regions, supported by the computation of the corresponding MSI values within these regions, reveals distinct qualitative trends. As it can be observed in the MSI values provided in Figure 5, while the sensitivity of the bifacial C_3 specimens' total reflectance to variations in the angle of incidence is markedly dominant in the visible

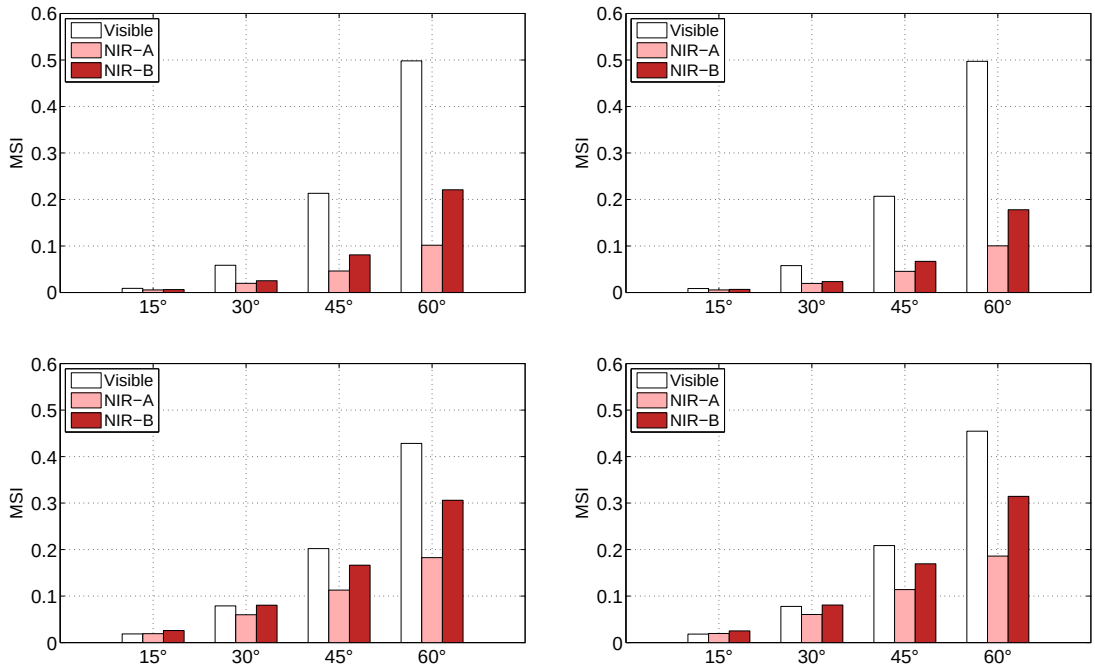

Figure 5: MSI values calculated for the total reflectance of the soy (top row) and maize (bottom row) specimens (obtained considering four angles of incidence: 15°, 30°, 45° and 60°) with respect to their total reflectance curve obtained considering normal incidence (0°). The curves for the soy and maize specimens were computed using the ABM-B[12] and ABM-U[13] models respectively. The characterization data employed for the soy specimens S1 (top left) and S2 (top right) as well as for the maize specimens M1 (bottom left) and M2 (bottom right) are provided in Table 1.

region, the sensitivity of the unifacial C_4 specimens' total reflectance is more balanced across the three spectral regions of interest.

Similar behaviours can also be observed with respect to the subsurface reflectance as depicted by the MSI values provided in Figure 6, albeit with distinct quantitative trends. More specifically, the sensitivity of the bifacial C_3 specimens' subsurface reflectance is more dominant in the visible region. For example, while the ratio of the visible and NIR-B MSI values computed for the bifacial C_3 specimens' total reflectance are equal to 2.6 (for S1) and 3 (for S2) considering an angle of incidence equal to 45°, the corresponding ratios for the bifacial C_3 specimens' subsurface reflectance is equal to 10 (for S1) and 11.15 (for S2). On the other hand, the sensitivity of the unifacial C_4 specimens' subsurface reflectance is slightly less balanced across the three spectral regions of interest. For example, while the ratio of the visible and NIR-B MSI values computed for the unifacial C_4 specimens' total reflectance is equal to 1.21 (for M1) and 1.23 (for M2) considering an angle of incidence equal to 45°, the corresponding ratio for the unifacial C_4 specimens' subsurface reflectance is equal to 1.37 (for M1) and 1.47 (for M2). We note that these quantitative trends are also verified for the other angles of incidence.

The success of remote sensing applications involving the discrimination and monitoring of crops depends on the correct understanding about the optical properties of the target species. Such an understanding, in turn, is derived from theoretical and applied investigations supported by measured foliar spectral data. Although this data is often obtained at low angles of incidence, the value set to this parameter may vary from one investigation to another, with values between 2.5° to 15° being commonly found in the literature[15,17,24–27]. In order to aggregate the results of these investigations in a meaningful manner, it is necessary to examine whether these angular differences may have a significant impact on the measured spectral quantities and how this impact may vary for the two main groups of cultivated species. For example, considering all reflectance curves obtained using an angle of incidence of 15° during this work, only the soy specimens' total reflectance had MSI values below 0.01 across the three spectral regions of interest (Table 2).

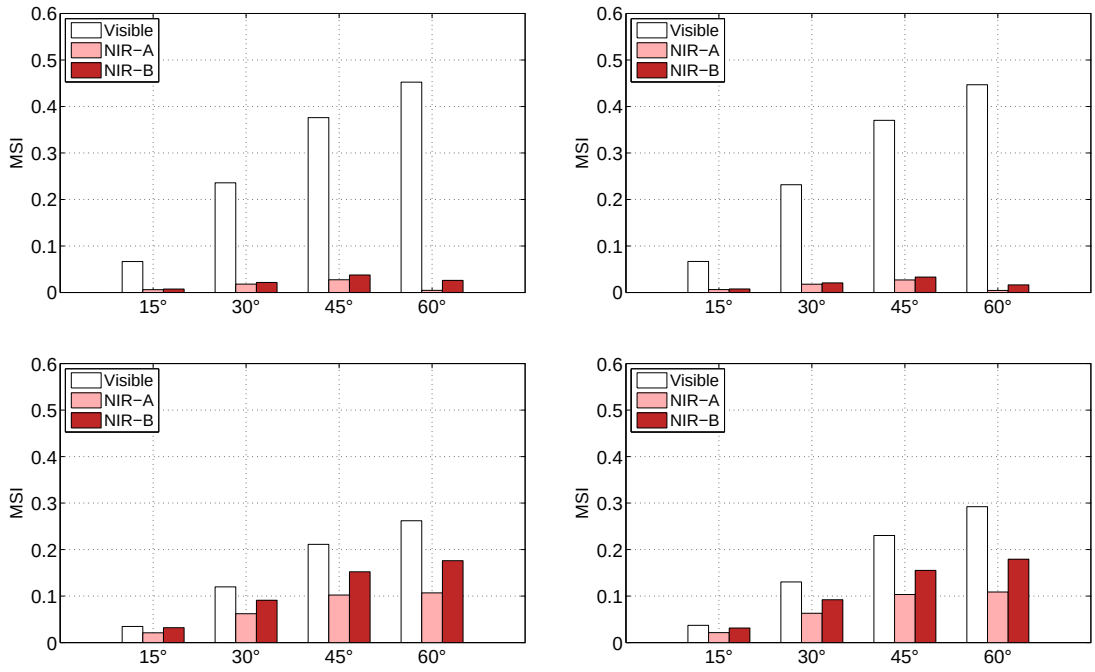

Figure 6: MSI values calculated for the subsurface reflectance of the soy (top row) and maize (bottom row) specimens (obtained considering four angles of incidence: 15°, 30°, 45° and 60°) with respect to their subsurface reflectance curve obtained considering normal incidence (0°). The curves for the soy and maize specimens were computed using the ABM-B[12] and ABM-U[13] models respectively. The characterization data employed for the soy specimens S1 (top left) and S2 (top right) as well as for the maize specimens M1 (bottom left) and M2 (bottom right) are provided in Table 1.

	total reflectance			subsurface reflectance		
Specimens	Visible	NIR-A	NIR-B	Visible	NIR-A	NIR-B
S1	0.0079	0.0055	0.0063	0.0665	0.0060	0.0073
S2	0.0076	0.0056	0.0067	0.0667	0.0062	0.0075

Table 2: MSI values associated with the bifacial C_3 specimens' total and subsurface reflectance curves obtained considering an angle of incidence of 15°.

While variations in the angle of incidence up to 15° had a negligible impact on the selected bifacial C_3 specimens' total reflectance, the same was not verified for the selected unifacial C_4 specimens. Similarly, these variations had a negligible impact (also illustrated by MSI values below 0.01 depicted in Table 2) on the selected bifacial C_3 specimens' subsurface reflectance for measurements performed in the NIR-A and NIR-B, which was not observed for the selected unifacial C_4 specimens either. In fact, to obtain similar MSI values for these specimens, we had to consider an angle of incidence of 5° (Table 3). These observations suggest that investigations based on bifacial C_3 specimens' reflectance responses will not be affected by variations on the angle of incidence as long as this angle does not exceed 15°. The same may not be applicable to unifacial C_4 specimens, however.

	total reflectance			subsurface reflectance		
Specimens	Visible	NIR-A	NIR-B	Visible	NIR-A	NIR-B
M1	0.0059	0.0034	0.0059	0.0139	0.0037	0.0076
M2	0.0062	0.0035	0.0064	0.0101	0.0039	0.0075

Table 3: MSI values associated with the bifacial C_4 specimens' total and subsurface reflectance curves obtained considering an angle of incidence of 5°.

It is also worth noting that the MSI values computed with respect to the NIR-A region were the lowest for all tested cases (Figures 5 and 6). We remark that, despite the significant morphological characteristics between bifacial C_3 and unifacial C_4 specimens, these plants share a similar dependence on the light absorbers present in their foliar tissues. For example, while their visible and NIR-B spectral responses are significantly affected by the presence of chlorophyll and water respectively, their NIR-A spectral responses are not[19]. Clearly, interpretations of experiments performed within this region are more likely to be applicable to both groups of specimens.

4. CONCLUSION AND FUTURE WORK

The *in silico* experiments described in this paper are by no means exhaustive, and any generalization regarding their outcomes may be premature. Nonetheless, our findings suggest that procedures devised to obtain information about plants' physiological status based on their hyperspectral responses should be flexible enough to account for the distinct morphological characteristics of plants belonging to C_3 and C_4 groups. Otherwise, the same procedure or apparatus capable of providing high-fidelity results for a plant belonging one group may lead to unreliable interpretations for a plant belonging to the other.

The effectiveness of indicators of plant's physiological status, such as the subsurface reflectance to transmittance ratio employed by Vanderbilt *et al.*,[6] depends on how these quantities are obtained, specially when multiple measurements are performed for different specimens. In these cases, small angular variations may introduce errors in the computation of these indicators. Our findings also suggest that, for measurements performed at more conspicuous low angles of incidence, the magnitude of these errors can be higher for unifacial C_4 specimens than for bifacial C_3 specimens. However, further analyses are required to determine the full extent of the sensitivity of bifacial C_3 and uniifacial C_4 specimens' hyperspectral responses to angular variations when measurements are performed considering an angle of incidence below 15°. Accordingly, as future work, we plan to expand our *in silico* experiments by considering not only other representative species belonging to the C_3 and C_4 groups, but also a higher angular sampling, notably for angles of incidence below 15°.

ACKNOWLEDGMENTS

This work was supported by the Natural Sciences and Engineering Research Council of Canada (NSERC-Discovery Grant 237337).

REFERENCES

[1] Disney, M., "Remote sensing of vegetation: potentials, limitations, developments and applications," in [*Canopy phosynthesis: from basics to applications*], K.Hikosaka, Niinemets, and Anten, N., eds., 289–232, Springer, Dordrecht (2016).

[2] Uto, K. and Kosugi, Y., "Hyperspectral manipulation for the water stress evaluation of plants," *Contemporary Materials* **III-I**, 18–25 (2012).

[3] Zarco-Tejada, P., Miller, J. R., Mohammed, G. H., l. Noland, T., and Sampson, P. H., "Vegetation stress detection through chlorophyll a+b estimation and fluorescence effects on hyperspectral imagery," *Journal of Environmental Quality* **31**, 1433–1441 (2002).

[4] Verrelst, J., Camps-Valls, G., Muñoz-Marí, J., Rivera, J., Veroustraete, F., Clevers, J., and Moreno, J., "Optical remote sensing and the retrieval of terrestrial vegetation bio-geophysical properties - A review," *ISPRS Journal of Photogrammetry and Remote Sensing* **108**, 273–290 (2015).

[5] Vanderbilt, V., Grant, L., and Ustin, S., "Polarization of light by vegetation," in [*Photon-vegetation interactions: Applications in optical remote sensing and ecology*], Nynemi, R. and Ross, J., eds., 191–228, Springer Verlag, Berlin, Germany (1991).

[6] Vanderbilt, V., Daughtry, C., and Dahlgren, R., "Relative water content, bidirectional reflectance and bidirectional transmittance of the interior of detached leaves during dry down," in [*IEEE International Geoscience & Remote Sensing Symposium - IGARSS*], (2015). Abstract.

[7] Baranoski, G., Chen, T., Kimmel, B., Miranda, E., and Yim, D., "On the high-fidelity monitoring of c3 and c4 crops under nutrient and water stress," in [*Asia-Pacific Remote Sensing Conference, Proc. of SPIE, Vol. 8524, Land Surface Remote Sensing*], Honda, D. E. Y., Sawada, H., and Shi, J., eds., 85240W–1–9 (2012).

[8] Muhaidat, R., Sage, T., Frohlich, M., Dengler, N., and Sage, R., "Characterization of $C_3 - C_4$ intermediate species in the genus *Heliotropium* L. (Boraginaceae): anatomy, ultrastructure and enzyme activity," *Plant, Cell & Environment* **34**, 1723–1736 (2011).

[9] Akhani, H., Ghasemkhani, M., Chuong, S., and Edwards, G., "Occurrence and forms of Kranz anatomy in photosynthetic organs and characterization of NAD-ME subtype C_4 photosynthesis in *Blepharis ciliaris* L. B. L. Burtt (Acanthaceae)," *Journal of Experimental Botany* **59**(7), 1755–1765 (2008).

[10] Baranoski, G., "Modeling the interaction of infrared radiation (750 to 2500 nm) with bifacial and unifacial plant leaves," *Remote Sensing of Environment* **100**, 335–347 (2006).

[11] Baranoski, G. and Eng, D., "An investigation on sieve and detour effects affecting the interaction of collimated and diffuse infrared radiation (750 to 2500 nm) with plant leaves," *IEEE Transactions on Geoscience and Remote Sensing* **45**, 2593–2599 (2007).

[12] NPSG, *Run ABM-B Online*. Natural Phenomena Simulation Group, University of Waterloo, Canada (2011). http://www.npsg.uwaterloo.ca/models/ABMB.php.

[13] NPSG, *Run ABM-U Online*. Natural Phenomena Simulation Group, University of Waterloo, Canada (2011). http://www.npsg.uwaterloo.ca/models/ABUB.php.

[14] Baranoski, G., Dimson, T., Chen, T., Kimmel, B., Yim, D., and Miranda, E., "Rapid dissemination of light transport models on the web," *IEEE Computer Graphics & Applications* **32**(3), 10–15 (2012).

[15] Hosgood, B., Jacquemoud, S., Andreoli, G., Verdebout, J., Pedrini, G., and Schmuck, G., "Leaf optical properties experiment 93," Tech. Rep. Report EUR 16095 EN, Joint Research Center, European Comission, Institute for Remote Sensing Applications (1995).

[16] Eng, D. and Baranoski, G., "The application of photoacoustic absorption spectral data to the modeling of leaf optical properties in the visible range," *IEEE Transactions on Geoscience and Remote Sensing* **45**, 4077–4086 (2007).

[17] Baranoski, G., Kimmel, B., Chen, T., and Yim, D., "In silico assessment of environmental factors affecting the spectral signature of C4 plants in the visible domain," *International Journal of Remote Sensing* **33**(4), 1190–1213 (2012).

[18] Krishnaswamy, A. and Baranoski, G., "A biophysically-based spectral model of light interaction with human skin," *Computer Graphics Forum* **23**(3), 331–340 (2004).

[19] Baranoski, G. and Rokne, J., [*Light Interaction with Plants: A Computer Graphics Perspective*], Horwood Publishing, Chichester, UK (2004).

[20] Baranoski, G., Rokne, J., and Xu, G., "Virtual spectrophotometric measurements for biologically and physically-based rendering," *The Visual Computer* **17**(8), 506–518 (2001).

[21] Hamby, D., "A review of techniques for parameter sensitivity analysis of environmental models," *Environ. Monit. Assess.* **32**, 135–154 (1994).

[22] Hamby, D., "A comparison of sensitivity analysis techniques," *Health Physics* **68**, 195–204 (1995).

[23] Hoffman, F. and Gardner, R., "Evaluation of uncertainties in radiological assessment models," in [*Radiological Assessment A Textbook on Environmental Dose Analysis*], Till, J. and Meyer, H., eds., 1–55, Division of Systems Integration, Office of Nuclear Reactor Regulation, U.S. Nuclear Regulatory Commision, NRC FIN B0766, Washington, DC, USA (1983). Chapter 11.

[24] Thomas, J., Namkem, L., Oerther, G., and Brown, R., "Estimating leaf water content by reflectance measurements," *Agronomy Journal* **63**, 845–847 (1971).

[25] Woolley, J., "Reflectance and transmittance of light by leaves," *Plant Physiology* **47**, 656–662 (1971).

[26] Al-Abbas, A., Barr, R., Hall, J., Crane, F., and Baumgardner, M., "Spectra of normal and nutrient-deficient maize leaves," *Agronomy Journal* **66**, 16–20 (1974).

[27] Maracci, G., Schmuck, G., Hosgood, B., and Andreoli, G., "Interpretation of reflectance spectra by plant physiological parameters," in [*International Geoscience and Remote Sensing Symposium - IGARSS'91*], 2303–2306 (1991).